Supplementary Information

Correlated cryogenic photoactivated localization microscopy and cryo-electron tomography

Yi-Wei Chang[1,2], Songye Chen[1,2], Elitza I. Tocheva[1], Anke Treuner-Lange[3], Stephanie Löbach[3], Lotte Søgaard-Andersen[3] & Grant J. Jensen[1,2,4]

[1]Division of Biology and Biological Engineering, California Institute of Technology, Pasadena, USA.
[2]Howard Hughes Medical Institute, Pasadena, USA.
[3]Max Planck Institute for Terrestrial Microbiology, Marburg, Germany.
[4]Correspondence should be addressed to G.J.J. (jensen@caltech.edu).

Nature Methods: doi:10.1038/nmeth.2961

Supplementary Figure 1 | Photoactivation/photoconversion of different PA-FPs at 80 K.

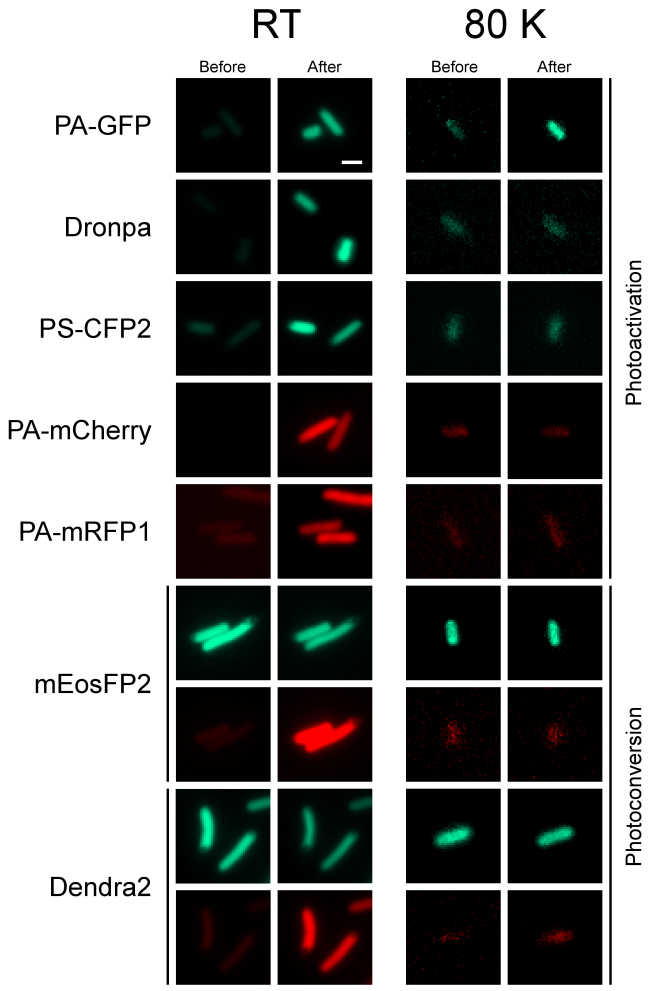

The two columns in the left panel show the photoactivation/photoconversion of PA-FPs in *E. coli* at room temperature. The two columns in the right panel show the results of photoactivation/photoconversion tests using the same samples at 80 K. The image brightness of different PA-FPs was optimized for signal visibility for each fluorophore, but is the same within each before/after pair. Note only PA-GFP maintained substantial photoactivatable properties at 80 K. Scale bar 1 μm. Representative images of five trials on each sample.

Nature Methods: doi:10.1038/nmeth.2961

Supplementary Figure 2 | Histograms of total numbers of photons detected from activated single PA-GFP molecules in the cryo-PALM images.

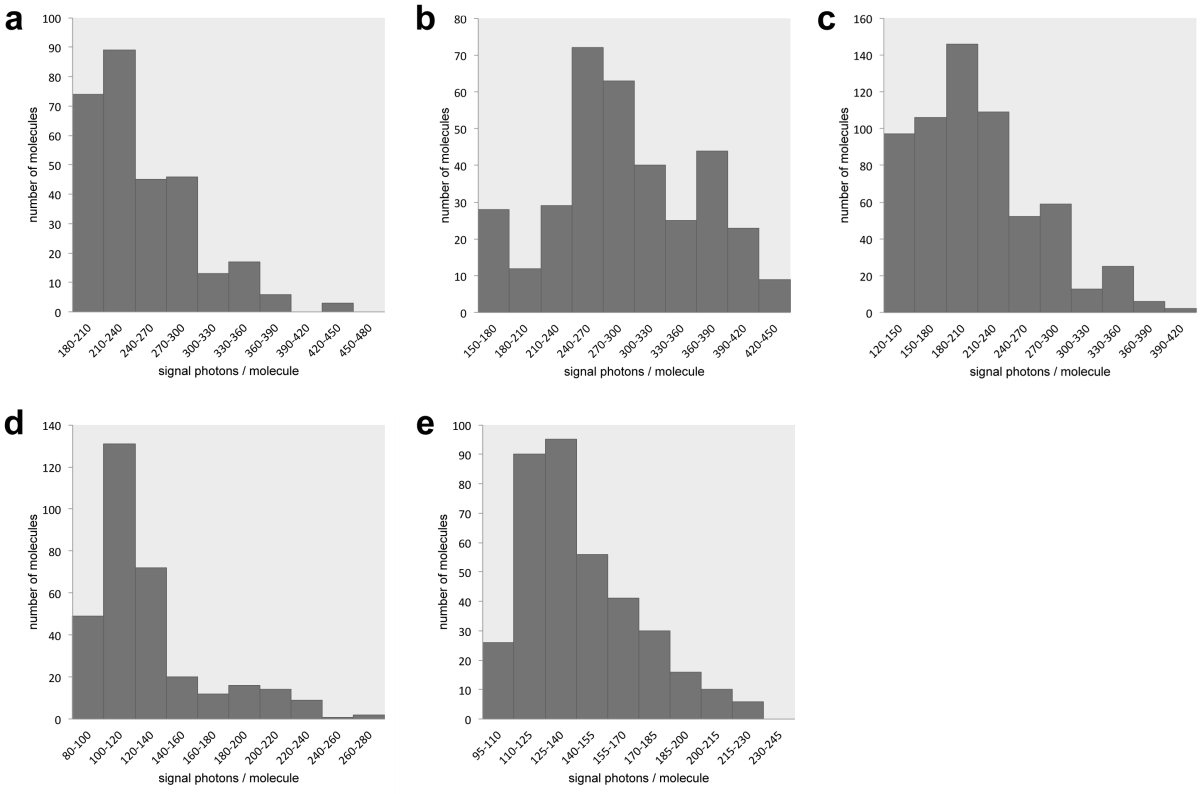

(**a**) Figure 1a, (**b**) Figure 1d, (**c**) Figure 2a, Supplementary Movie 2, (**d**) Figure 2e and (**e**) Supplementary Movie 1. The average number of photons collected per blinking PA-GFP molecule is 206.

Nature Methods: doi:10.1038/nmeth.2961

Supplementary Figure 3 | Preventing laser-induced ice crystallization.

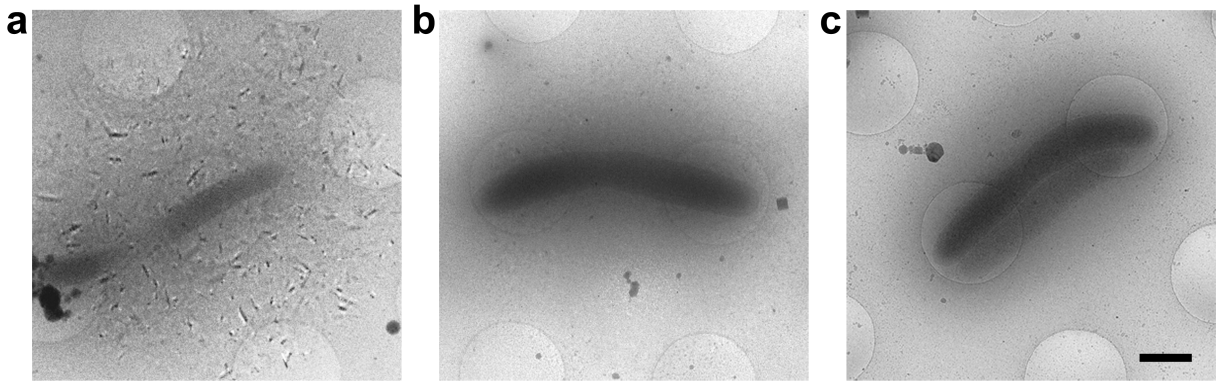

Cryo-EM images of *M. xanthus* cells (**a**) frozen on an EM grid in CTT culture medium and exposed to the cryo-PALM laser for 150 seconds; (**b**) frozen on an EM grid in CTT medium containing 5% Ficoll PM 70 and exposed to the laser for 300 seconds; (**c**) frozen on an EM grid in CTT medium containing 10% Ficoll PM 70 and 10% ethylene glycol and exposed to the laser for 300 seconds total, with 60 seconds rest after every 60 seconds exposure. In all cases, the laser was adjusted to an intensity of 300 W/cm^2 on the sample and spread over an area of ~100 μm^2. Scale bar 1 μm.

Nature Methods: doi:10.1038/nmeth.2961

Supplementary Figure 4 | Immunoblot analysis of Hcp and fluorescently-labeled VipA accumulation in total cell extracts and supernatants of the indicated genotypes.

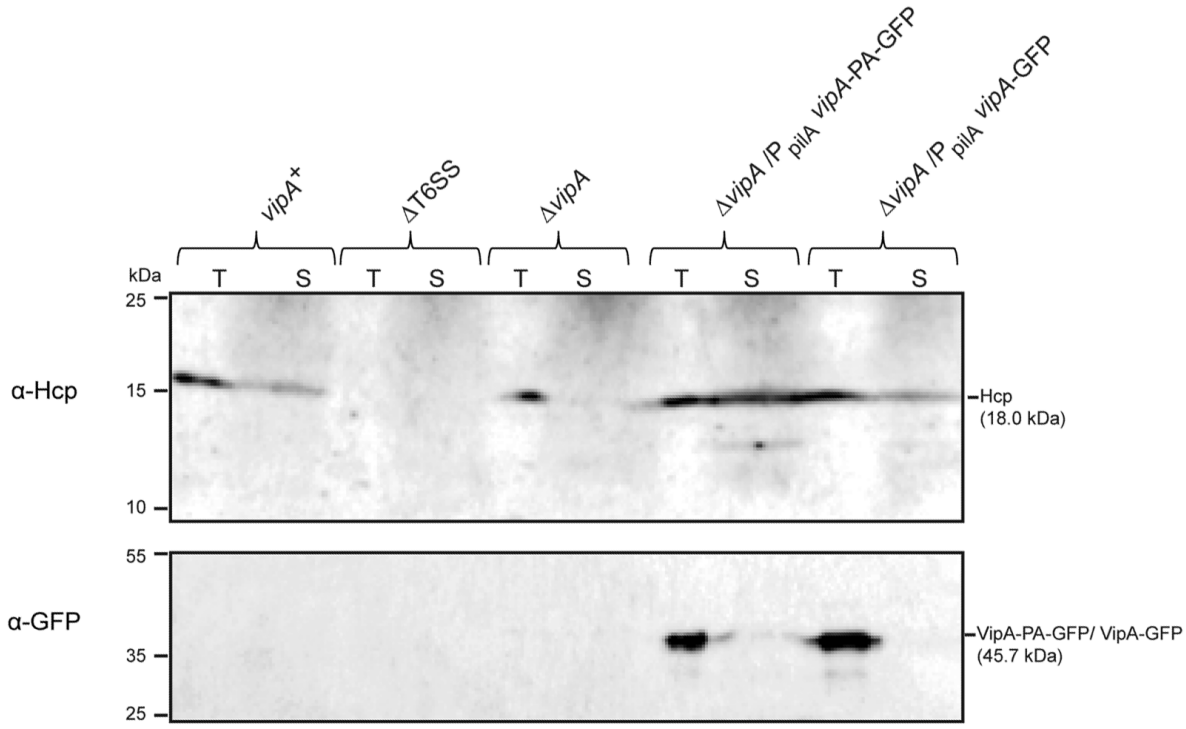

Total cell extract (T) from $2.5x10^7$ cells and cell-free supernatant (S) from $1.5x10^{10}$ cells were loaded. The blots were probed with α-Hcp to generate the upper panel. The α-Hcp was then stripped away and the same membrane was probed with α-GFP to produce the lower panel. Positions of Hcp, VipA-PA-GFP, and VipA-GFP with their calculated molecular mass, and molecular markers are indicated.

Nature Methods: doi:10.1038/nmeth.2961

Supplementary Figure 5 | Comparison of fluorescent images from room temperature FLM, cryo-FLM, and cryo-PALM.

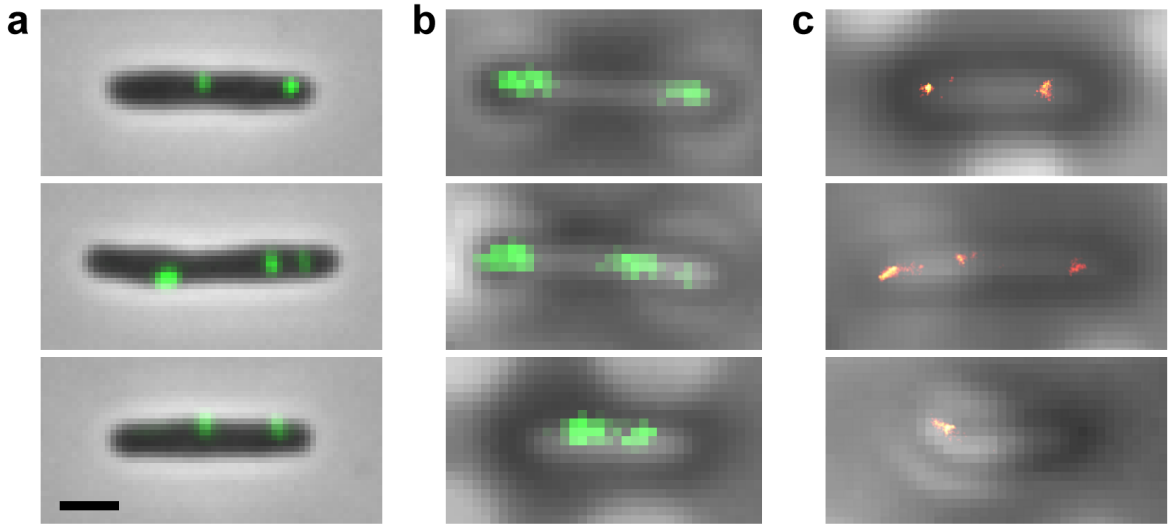

(**a**) *M. xanthus* SA4137 (Δ*vipA* strain containing VipA-GFP) cells on a coverslip imaged with a 100x, NA 1.4 oil immersion objective lens at room temperature. (**b**) *M. xanthus* SA4137 cells frozen on an EM grid imaged with a 60x, NA 0.7 air objective lens at 80 K. (**c**) Cryo-PALM images of *M. xanthus* SA5718 (Δ*vipA* strain containing VipA-PA-GFP) cells frozen on an EM grid at 80 K. Upper panel: $(\sigma_{x,y})_{max}$ = 220 nm, M_{image} = 395; middle panel: $(\sigma_{x,y})_{max}$ = 180 nm, M_{image} = 1148; lower panel: $(\sigma_{x,y})_{max}$ = 170 nm, M_{image} = 308. Phase contrast images revealing cell outlines are superposed in grayscale for all images. GFP signals in **a** and **b** are shown in green. PA-GFP locations in **c** are shown by color gradient, yellow (high precision) to red (low precision). Scale bar 1 μm.

Nature Methods: doi:10.1038/nmeth.2961

Supplementary Figure 6 | Reducing stage vibrations through enhanced cryo-FLM stage insulation.

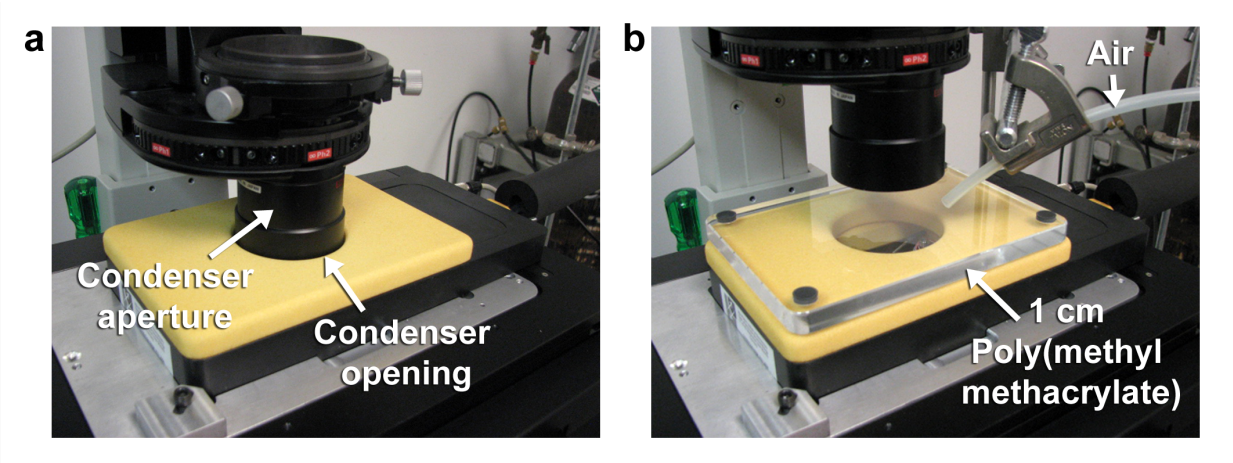

(**a**) Original design of the FEI CryoStage[2]. The room-temperature condenser aperture needs to be inserted into the cryo-stage through a "condenser opening" hole in the insulating lid (yellow). (**b**) Modified cryo-stage. A 1-cm thick poly(methyl methacrylate) plate was introduced to reduce heat loss through the hole but preserve transparency for light traveling through the condenser aperture into the cryo-stage. A continuous air stream was directed onto the poly(methyl methacrylate) plate in order to prevent water condensation.

Nature Methods: doi:10.1038/nmeth.2961

Supplementary Figure 7 | Cryo-PALM-CET alignment precision.

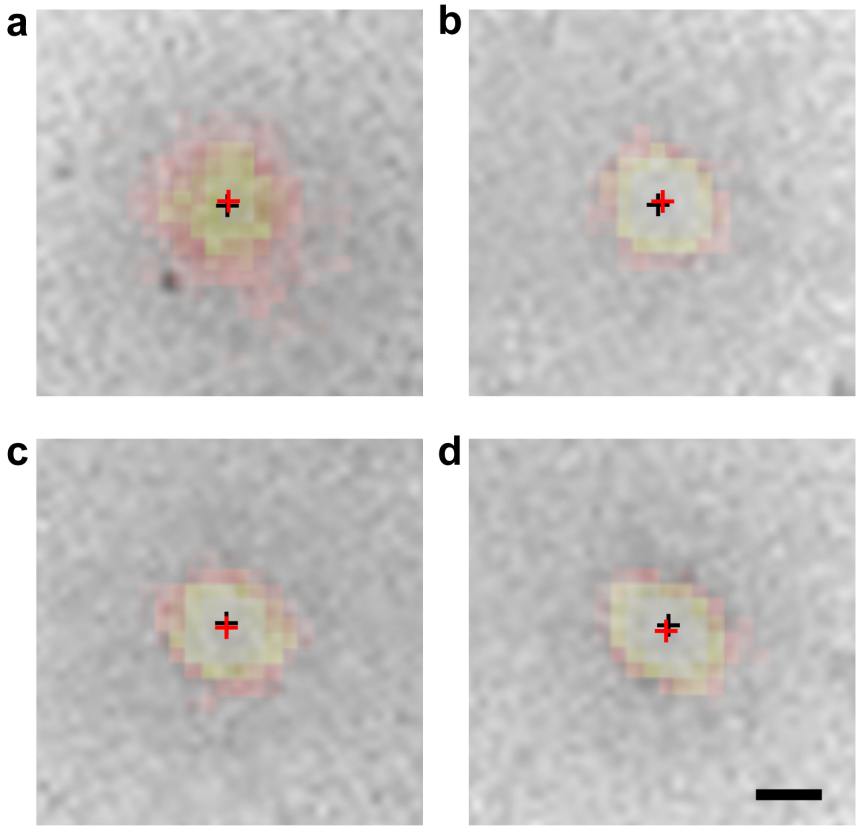

Superposed cryo-PALM (foreground with yellow to red color gradient) and EM (grayscale background) images of the fluorescent beads located in the (**a**) upper-left, (**b**) upper-right, (**c**) lower-left, and (**d**) lower-right corners of Supplementary Movie 1. Black and red cross symbols indicate bead centers in EM and cryo-PALM images, respectively. The distances between the centers of the same bead in the two images are 9 ± 2 nm. Scale bar 100 nm.

Nature Methods: doi:10.1038/nmeth.2961

Supplementary Table 1 | Parameters of merit for the acquisition and analysis of the cryo-PALM images.

	τ_{frame} (ms)	F_{total}	Image size (μm^2)	M_{total}	$(\sigma_{x,y})_{max}$ (nm)	M_{image}
Figure 1a	100	400	1.05 x 1.05	386	160	294
Figure 1d	100	500	1.05 x 1.05	525	160	345
Figure 2a, Supplementary Movie 2	100	500	1.05 x 1.05	830	160	617
Figure 2e	100	500	1.05 x 1.05	473	180	327
Supplementary Movie 1	100	500	1.05 x 1.05	557	200	370

τ_{frame} = acquisition time for each frame of the image stack; F_{total} = total number of acquired frames in the image stack; M_{total} = total number of molecules localized in the image stack; $(\sigma_{x,y})_{max}$ = maximum acceptable position error for inclusion in the final image; M_{image} = number of localized molecules comprising the final image.

Nature Methods: doi:10.1038/nmeth.2961

Supplementary Table 2 | *M. xanthus* strains used in this work.

Strain name	**Genotype**	**Reference**
DK1622	wild-type	[22]
SA5707	ΔT6SS (*ΔMXAN4800-MXAN4813*)	This work
SA5716	Δ*vipA* (*ΔMXAN4807*)	This work
SA5718	Δ*vipA*/P_{pilA}-*vipA*-PA-GFP (*attB*::pSlo5)	This work
SA4137	Δ*vipA*/P_{pilA}-*vipA*-GFP (*attB*::pMAT36)	This work

Nature Methods: doi:10.1038/nmeth.2961

Supplementary Table 3 | Primers used in this work.

Primer	Sequence[a]
oVipA1	**CTAGTCTAGA**AGCAAAGAGAGTTCCGTCGCC
oVipA3	**CGCGGATCC**CTTGGTCTCTTCGGTCAGACC
oGFP1	**GCGCGGATCCGCGGCGGCCGGGGGCGGG**ATGGCCAAGGGCGAGGAGCTG
oGFP2	**GCGCGGTACC**TTACTTGTACAGCTCGTCCA
oPAGFP1	**CGCGGATCCGCGGCGGCCGGGGGCGGG**GTGAGCAAGGGCGAGGAG
oPAGFP2	**CGGGGTACC**TTACTTGTACAGCTCGTCCATGCC
mxan4807A	**ATCGCAAGCTT**AGACGCTCATCTCCACCTTGGGAAGC
mxan4807B	**ACTCGGGATCC**GGTAGGGGCGACGGAACTCTCTTTGC
mxan4807C	**ACTCGGGATCC**GAACTGGGTCTGACCGAAGAGACC
mxan4807D	**TAGCGTCTAGA**AAGCTCTCCTCGCCGAACACTTCC
mxan4800A	**ATCGCAAGCTT**CGAACATCTCCAGCGACG
mxan4800B	**ATCGCGAATTC**CTCTCCGGCGGTGAAGGG
mxan4813C	**ATCGCGAATTC**CTGCATGTGGCCCTGACC
mxan4813D	**TAGCGTCTAGA**GGCCTGCGCCTTGCTGG

[a]Primer sequences that are not complementary to the template are indicated in bold.

Nature Methods: doi:10.1038/nmeth.2961